

The Australian Summer Monsoon

Harry Hendon

BMRC

With contributions from

Matthew Wheeler and John McBride

BMRC

Introduction

The Australian summer monsoon is traditionally referred to as the wet season in Northern Australia when over three-quarters of the annual rainfall occurs. The Australian summer monsoon is just a portion of the greater Australian-Indonesian Monsoon that extends from the equator to about 15°S and westward from 100°E to about 155°E. The greater Austral-Indonesian monsoon is unique because it develops over the “Maritime Continent”, which is essentially ocean covered. A case has been made, in fact, that the Australian monsoon would exist even in the absence of any forcing due to land-ocean contrast (Yano and McBride 1998). Nonetheless, the monsoon over Australia evolves in a fashion characteristic of other continental monsoons. This includes seasonal reversal of tropospheric circulation (Fig. 1 from Hung et al. 2004), development of a monsoon (thermal) trough, and rapid onset. And, similar to its Indian-Asian counterpart, the monsoon exhibits strong intraseasonal variations but relatively weak (compared to the mean) interannual variations. Here we touch on aspects of the onset process, the role of the MJO for intraseasonal and interannual variability, and the impact of ENSO.

Broadscale Evolution

In the traditional view, sensible heating over the continent, which leads to a reversal of the lower tropospheric meridional temperature gradient (warmer over land to the south than over the ocean to the north), ultimately drives the Australian monsoon. A thermally induced meridional circulation then develops (i.e., a giant sea breeze; e.g., Hung and Yanai 2004). Low level onshore north-westerlies transport moist air inland, which allows the monsoon to expand poleward over arid northern Australia. In conjunction with development of the monsoon trough, lower tropospheric westerlies and associated widespread rainfall replace the dry-trade easterlies that predominate during winter. Onset of the monsoon, typically in late December, also coincides with a rapid poleward contraction of the subtropical jet and ridge (Fig. 2, from Hendon and Liebmann 1990a). After onset the trade easterlies strengthen south of the trough and upper tropospheric easterlies develop, yielding a tropical circulation with a deep baroclinic structure. Along about 10–15°S a line of strong cyclonic ($-\partial u/\partial y$) shear separates lower latitude westerlies from higher latitude easterlies (McBride and Keenan, 1982). The monsoon typically retreats by April.

Bursts, Breaks, and Intraseasonal Variability

The monsoon is composed of bursts and breaks that typically last 1-3 weeks (Fig. 3, from Wheeler and McBride 2004). Onset typically coincides with beginning of an active burst. The burst and breaks are often a reflection of passage of the Madden-Julian Oscillation (MJO; e.g., 1987/88). But, the MJO is not the only source of intraseasonal variability nor is it the trigger for every onset.

The role for the MJO in driving monsoon variability is quantified by spectral analysis of zonal at 850 mb at Darwin and northern Australia rainfall (Fig. 4, from Hendon and Liebmann 1990b). A spectral peak in the MJO band (30-70 days) in zonal wind is evident, but not in

rainfall. The peak in zonal wind only stands out above the background spectrum (here subjectively determined by averaging across frequencies adjacent to the MJO band) by about a factor of 0.5. That is, the MJO signal only accounts for about 1/3 of the zonal wind variance in the 30-70 day range. No peak is evident in rainfall, which reflects the much noisier nature of convective rainfall even after spatial averaging. However, rainfall is coherent with zonal wind in the 30-70 day band. Rainfall leads westerly wind by a few days, which is typical of the MJO. Thus, the MJO clearly impacts variability of the monsoon, but usually in only a modest fashion.

While the MJO may only play a modest role in the monsoon when all years are considered together, there are clearly times that the MJO dominates monsoon variability. The role of the MJO in the monsoon is elucidated by objectively identifying the MJO from global analyses and then comparing the monsoon variations to those associated with the MJO. Wheeler and Hendon (2004) objectively defined the MJO by combined EOF analysis of equatorial averaged zonal wind at 200 and 850 mb and OLR. A dominant leading pair of modes is associated with the MJO. The typical structure of the MJO in the Australian monsoon is revealed by composites that are based on the phase of the MJO as given by the projection onto these leading two EOFs (Fig. 5, from Wheeler and Hendon 2004). Suppressed conditions exist at phase 1 and 2 (phases are separated by about 1 week), with anomalous easterlies across and to the north of northern Australia. Active convection commences at phase 4, with monsoonal westerlies becoming established by phase 5. An interesting tropical-extratropical teleconnection is evident in southwestern Australia at Phase 3, whereby enhanced convection there occurs ahead of the low-level cyclone before convection becoming established to the north at Phase 4. By Phase 7, the active convection has moved off to the east. At Phase 8 the monsoonal westerlies have decayed and suppressed conditions are reestablished. This entire cycle takes on the order of 30-50 days.

Locally at Darwin, the amplitude of the oscillation at Darwin is about 5 ms^{-1} in zonal wind, 0.75 ms^{-1} in meridional wind, 5 mm rainfall per day, and 10% in relative humidity (Fig. 6 from Hendon and Liebmann 1990b). The deep baroclinic structure in zonal wind has its node at about 300 hPa. The temperature structure is similar to that described by McBride and Frank (1999), with a warm anomaly of the order of 0.9 K in the upper troposphere and a cold anomaly of similar size in the lower troposphere. Boundary layer relative humidity increases about 1 week prior to commencement of active convection. This feature, which may result from a slow vertical build up of convection that progressively moistens and deepens the boundary layer, may reflect a process critical to the dynamics of the MJO and which may be absent in many GCMs.

A concrete measure for the role of the MJO in each years' monsoon is provided by the multiple correlation coefficient squared, R^2 , between the 3-day running-mean OLR anomaly across northern Australia and the projection coefficients onto Wheeler and Hendon's leading pair of EOFs (values indicated in middle right of each panel in Fig. 3). Nearly 60% of the OLR convective variability in the 1987/88 monsoon can be accounted for by the MJO, while in 1982/83 this drops to less than 10%. Some of this interannual variability is likely related to interannual variability in the strength of the MJO itself (e.g., Hendon et al. 1999). That is, the variability in the monsoon that is accounted for by the MJO is proportional to the tropically averaged level of MJO activity.

Monsoon variability is also associated with large-scale westward propagating disturbances (McBride 1983; Davidson et al. 1983; Keenan and Brody 1988; Hendon et al. 1989). Although it can be quite varied, the phase speed of the westward convective envelopes is often about the same, except in the opposite direction, as that of the eastward MJO ($\sim 5 \text{ m s}^{-1}$). Usually the westward envelopes are maximized off the equator, and can be accompanied by large variations in the rotational wind as well. Such characteristics are suggestive of an influence on the monsoon

by equatorial Rossby (ER) waves (e.g., Matsuno 1966). The structure and evolution of the typical ER wave in the Australian region is displayed in Fig. 7 (from Wheeler et al. 2000). The symmetric circulation cells on either side of the equator are clearly seen, though in individual cases symmetry is hard to detect.

Such westward propagating ER waves were evident during the 1986/87 monsoon. Hovmoller plots of zonal and meridional wind at 850 mb are displayed in Figs. 8 and 9. The waves are detectable as far east as the date line. Also indicated in these figures are the tracks of the tropical cyclones that developed, which are located in the troughs of these disturbances in both hemispheres. As will be discussed in the next section, onset of the monsoon this year also seems to be triggered by arrival of one of these troughs.

Another potential source of variability within the monsoon is the cross-equatorial influence of cold surges in the South China Sea. These surges are characterized by periods (order several days) of strong cross-equatorial northerly winds, anomalously low temperatures, and an increase in surface pressure in the South China Sea. Compo et al. (1999) found submonthly (6–30 day) time-scale surges were directly related to convective activity south of Indonesia. Sumathipala and Murakami (1988), on the other hand, found no contribution of lower-frequency, 30–60 day, northerly surges of east-Asian origin to convection in the Australian-Indonesian monsoon. Instead, they found a contribution from northeasterly flows originating in the subtropical north Pacific.

Thermodynamic Changes and Triggers of Onset

From a local thermodynamic perspective, onset involves a gradual built up of low level moist static energy and CAPE, but with significant convective inhibition. For example, in November and December 1986 pre-monsoon conditions existed (Fig. 10, from Hendon et al. 1989), with

large CAPE and strong mid-troposphere static energy minimum but dry boundary layer. The build up of low-level moist static energy and CAPE results primarily from an increase in surface temperature. CAPE is not realized prior to onset due to strong convective inhibition from a lack of lower tropospheric humidity. That is, parcels would have to be lifted more than 100 mb from the surface to become buoyant prior to onset. The AMEX experiment in January 1987 experienced an active monsoon. Widespread, deep convection acts to increase mid-tropospheric temperature, decrease lower tropospheric temperature and reduce CAPE. But, the increase in low level humidity also leads to dramatically reduced convective inhibition. McBride and Frank (1999) describe a similar contrast between active and break episodes of the monsoon.

These changes in stratification before and after onset are also reflected in the changes in the characteristics of convection. Convection during the premonsoon (and break periods) is less widespread but has higher vertical development, higher reflectivity above the melting level, a lack of large stratiform decks, more intense updrafts, and higher electrical activity (e.g., Keenan and Carbone 1992). In comparison, convection during the active westerly monsoon is widespread with weaker updrafts and often associated with squall-like structures within large mesoscale stratiform decks (e.g., Keenan and Rutledge 1993). Thus, while active monsoon conditions result in more widespread rain, the individual convective cells involved are generally less intense. To some extent these differences can be attributed to a continental as compared to maritime source of the airstream in which the convection is embedded. The active monsoon tends to have low level flow from the north (onshore), while the premonsoon and break periods experience flow from the south (off the continent). However, such differences in convective characteristics are also consistent with the general large-scale static stability changes discussed by Hendon et al. (1989) and McBride and Frank (1999).

While the switch from dry, south-easterlies to wet north-westerlies is sudden, sensible heating from the ground surface, which contributes to the creation of the land-sea thermal contrast in the Australian sector, is gradual and begins as early as September (Hung and Yanai 2004). Hence, some other trigger is required to instigate the sudden onset. Possible candidates include passage of the convective phase of the MJO or other synoptic-scale tropical waves that produce moist northwesterly flow and lower tropospheric convergence (e.g., Davidson et al. 1983; Hendon et al. 1989) and penetration of extratropical troughs that perhaps act to destabilize the upper troposphere (e.g. Davidson et al. 1983; Hung and Yanai 2004).

A case for the role of the MJO in the onset of the monsoon can be made by compositing daily OLR and other meteorological variables relative to a subjectively defined onset date. Unfortunately, determination of onset date is not unique and subsequent interpretation depends on the definition of onset. Hendon and Liebmann (1990a) defined onset as the first occurrence of broad-scale wet conditions in northern Australia in conjunction with westerly 850 mb winds at Darwin, based on weakly low pass filtered daily data (i.e., periods shorter than 3-4 days were removed). The composite evolution of zonal wind about onset is consistent with that produced by the MJO: onset coincides with development of deep westerlies overlain by upper tropospheric easterlies that persist for about 2-3 weeks. The evolution of OLR for the composite onset (Fig. 11, from Hendon and Liebmann 1990a) reveals that onset is associated with the slow eastward propagation of convection from the Indian Ocean that typifies the MJO. At Australian longitudes, low OLR (enhanced convection) dips southward at onset and then retreats equator as the convective phase passes into the western Pacific. Hendon and Liebmann (1990a) note, however, that the standard deviation of these composite OLR anomalies is as large as the composite itself. Thus, the role of the MJO is not necessarily dominant. By taking a more local

view of the monsoon onset (i.e. development of deep westerlies at Darwin), Drosowsky (1996) made the case that the MJO was no more important than any other synoptic variability.

Wheeler and Hendon (2004) re-examined the relationship between monsoon onset and the state of the MJO, as defined by the leading pair of EOFs of equatorial averaged zonal wind and OLR (Fig. 12, from Wheeler and Hendon 2004). Onset dates were determined by Drosowsky (1996). When the MJO is strong, onset occurs more than 80% of the time when the MJO is in Phases 4–7 (i.e., when MJO low-level westerlies and broad-scale convection are in the vicinity of northern Australia) and less than 20% of the time in all the other phases (i.e., when northern Australia is in the suppressed phase of the MJO). The spread of onsets from Phases 4 to 7 covers a time window of half the period of the MJO (i.e., about 20 to 30 days), which is significantly greater spread than the ± 4 days found by Hendon and Liebmann (1990a). However, Hendon and Liebmann used a “local” definition of the MJO (i.e. low pass filtered (periods shorter than about 3 days removed) winds and rainfall in the Australian sector), which clearly captures variability besides that due to the MJO. Thus, it appears that the MJO limits monsoon onset to within its active half-cycle, but the actual onset is often set by other, presumably shorter time-scale, phenomena. This view is consistent with Hung and Yanai (2004) and the earlier study of Hendon et al. (1989), both of who found the large-scale, low-frequency, influence of the MJO to be only one of a number of factors that determine onset.

In their study of the monsoon onset during Winter MONEX, Davidson et al. (1983) presented evidence that the trigger mechanism for onset lay in the evolution of synoptic-scale weather disturbances to the south and west of Australia. They hypothesized that prior to onset the seasonal buildup of planetary-scale and land-sea temperature gradients reaches a critical stage.

Before the onset can take place, however, traveling highs and lows (“weather systems”) to the south must be configured so that trade easterlies are prevalent across the Australian continent .

The case for triggering of onset by westward propagating, equatorial Rossby waves was made by Hendon et al. (1989). As previously mentioned, onset of the monsoon during the 1986/87 season coincided with arrival of the trough of one such Rossby wave (Figs. 8 and 9). Furthermore, another packet of Rossby waves some 3 weeks later also seems to explain revival of the monsoon.

Danielsen (1993) proposed a mechanism whereby the passage of midlatitude cold fronts south of the Australian continent spread cold air northward across the continent, which in turn interacted with the continental scale sea-breeze lying across the northern part of the continent. Such a description bears much similarity to that for the South China Sea cold surges (e.g., Love 1985). Danielsen showed that changes in lower-tropospheric stability and low-level convergence contribute to the triggering of convection and were synchronized with the passages of these higher latitude cold fronts.

Kawamuura et al. (2002) propose that onset involves an air-sea feedback, in much the same fashion as discussed by Nicholls (1981), Hendon (2003), and Wang et al. (2003) in the context of the SST evolution north of Australia during ENSO. Kwamauura et al. suppose that the initial sensible heating of the continent prior to monsoon onset acts to drive shallow north-westerly onshore flow, which superimposes on the mean easterly trades to the north of Australia. Thus, windspeed is reduced, thereby reducing latent heat flux and ocean mixing, hence increasing local SST. Warm SST then promotes stronger north westerly flow (i.e., akin to a Gill (1980) response to an imposed heat source), further reducing the windspeed and warming the SST. Warm SST acts to enhance convective instability , which continues to build up until onset.

Onset of the monsoon, in their view, still requires an additional trigger, for instance the passage of the MJO.

Modulation of synoptic weather

Modulation of synoptic weather (including likelihood of extreme rainfall events) by lower frequency intraseasonal variability is also observed in the monsoon. Enhanced transient kinetic energy at Darwin accompanies the wet phase of the MJO, along with enhanced rainfall variance (Hendon and Liebmann 1990b). The enhanced kinetic energy occurs through the depth of the troposphere but with maxima around 850 hPa and 100 hPa, consistent with the baroclinic structure that is common to many tropical systems. Liebmann et al. (1994) also showed a roughly 2:1 modulation of tropical cyclones between wet and dry MJO phases in the Indian and western Pacific sectors (also Hall et al. 2001). The hypothesis for such a modulation is that the large-scale MJO anomalies alter the climatologically favourable factors for TC development (e.g. low-level cyclonic vorticity, low vertical wind shear; Gray 1979) on a time-scale that is slow enough that they act in the same way as those climatological base-state factors.

Interestingly, the modulation of TC numbers by low-frequency (relative to the TC) variability is not restricted to the MJO band. A higher and lower frequency bands produce the same degree of modulation. Hence any form of low-frequency (relative to the TC), large-scale variability that alters the dynamical factors favorable for cyclogenesis appears to modulate TC activity.

Wheeler and Hendon (2004) also observed modulation of extreme continental rainfall during the summer monsoon by the MJO. They looked at the contemporaneous relationship between the occurrence of the highest quintile of weekly rainfall across Australia and the phase of the MJO. The normal probability of a weekly rainfall total in DJF being in the upper quintile is, by

definition, 20%. Across the Top End region (around Darwin), the probability varies from less than 12% in Phases 1 and 2 (suppressed phase of MJO) to greater than 36% in Phases 5 and 6 (active phase of MJO). This represents more than a tripling of the likelihood of extreme rainfall from the dry to wet phase of the MJO.

Interannual Variability and ENSO

ENSO exerts considerable influence on Australian rainfall, but the weakest impact is during the summer season (Fig. 13 from McBride and Nicholls 1983,; see also Holland 1986). Summer monsoon rainfall is modestly correlated with El Niño (~-0.4), but the bulk of this negative correlation comes from a strong negative correlation in the transitional season (Sep-Nov; Table 1 from Nicholls et al. 1982). Once the monsoon is active, the correlation of wet season rainfall and ENSO is near zero.

Similarly, onset of the summer monsoon, as defined by date of the first 250 mm of rainfall at Darwin, is negatively correlated with El Niño (late onset during warm events, when pressure is high at Darwin; Fig. 14 from Nicholls et al. 1982). Because of strong persistence of ENSO anomalies from June through November, onset of the Australian summer monsoon is predictable some months ahead. But, total wet season rainfall is not correlated with onset date (Table 1 from Nicholls et al. 1982). Interestingly, onset date as defined by the first 250 mm of rainfall (which is about ¼ of the wet season total) is 3 weeks earlier than onset as determined by the large-scale rearrangement of the tropical circulation. Thus, the strong negative correlation of El Niño with onset date and transitional season rainfall occurs before the summer monsoon circulation is established (i.e., when northern Australia is still in a trade wind regime).

Because of persistence of ENSO anomalies from June-November, onset date of the monsoon is also related to the strength of the previous Indian monsoon (Fig. 15, from Joseph et al. 1991).

A weak Indian summer monsoon tends to occur during a developing El Niño, which is then followed by a late onset of the Australian summer monsoon. Joseph et al. point out that the relationship between the strength of Indian monsoon and onset date of the Australian summer monsoon seems to hold even in the absence of ENSO. They suggest that the Indian summer monsoon is capable of driving SST variations (warm in the western Indian Ocean and cold to the north of Australia), which subsequently act to delay onset of the Australian monsoon. Such possible behavior needs to be explored in coupled models with ENSO artificially suppressed.

Hung et al. (2004) further emphasize that the Australian summer monsoon is not related to the following Indian monsoon, which reflects both the lack of persistence of ENSO after December and lack of simultaneous relationship of the Australian summer monsoon and ENSO. They argue that the Australian summer monsoon acts to disrupt the ENSO cycle.

Insight into why the ENSO influence on the Australian summer monsoon wanes at the peak of the monsoon is gained by examination of the seasonal evolution of SST anomalies through the ENSO cycle (Fig. 16 from Hendon 2003). In southern winter (JJA) and spring (SON) of an El Niño year, SSTs are cold to the north of Australia and winds are anomalously easterly. These cold SSTs reinforce anomalous subsidence driven by the warm equatorial SSTs in the central and eastern Pacific. Hence, dry conditions in northern and eastern Australia tend to prevail in winter and spring. But, in DJF (summer), despite persistence of warm anomalies in the Pacific and the associated easterly anomalies to the north of Australia, the cold SSTs to the north of Australia disappear. The reinforcement they provide to the remotely forced subsidence thus ends.

The evolution of the SST anomalies to the north of Australia has been postulated to stem from seasonally varying air-sea feedback in the region (Nicholls 1981, Hendon 2003, Wang et al. 2003). During the winter (JJA) and spring (SON), the region experiences trade easterlies. In the mean, they act to elevate the thermocline in the eastern equatorial Indian Ocean and to

promote upwelling along the Java/Sumatra coast. In other words, in the mean the easterlies produce conditions favorable for air-sea coupling. Anomalous easterlies (for instance, driven remotely by El Niño in the Pacific) at this time of year, then would act to 1) increase the total windspeed (easterly anomaly acting on an easterly basic state) thereby producing surface cooling through increase latent and sensible heat flux and 2) further elevate the thermocline in the east and promote enhanced upwelling on the Java/Sumatra coast thereby producing more surface cooling in the eastern Indian Ocean. Thus, a positive feedback is produced with colder SST anomalies acting to raise surface pressure in the eastern Indian Ocean and producing stronger easterly anomalies. Once the Australian summer monsoon onsets and the mean winds become westerly, the thermocline in the east deepens and mean upwelling along the Java/Sumatra coast ceases. Anomalous easterlies now acting on a westerly basic state now will decrease the total windspeed, thereby acting to warm the surface. Hence, together with the lack of communication of the subsurface anomalies to the surface (because the mean thermocline is too deep and coastal upwelling is weak), the easterly anomalies will produce a negative feedback. The positive feedback during the winter and spring and negative feedback during summer is offered as an explanation for the strong correlation between onset date and El Niño but for a weakening of the negative correlation between El Niño and northern Australia rainfall once the monsoon onsets.

Other sources of interannual variability of the summer monsoon include seasonal variations of MJO activity. Hendon et al. (1999) show years of strong MJO activity tend to occur when convection over Australia is suppressed. That is, years of strong MJO activity tend to be years with a weak summer monsoon. Seasonal MJO activity shows little relationship with ENSO (or any other SST anomalies). Hence, the seasonal rainfall variance accounted for by the level of MJO activity is independent of that accounted by ENSO. However, as the level of MJO activity

is not obviously related to SST boundary forcing (Hendon et al. 1999, Slingo et al. 1999), it is not clear that the MJO-induced component of seasonal monsoon variability will be predictable.

References

- Compo, G.P., G.N. Kiladis, and P.J. Webster, 1999: The horizontal and vertical structure of east Asian winter monsoon pressure surges. *Quart. J. Roy. Meteor. Soc.*, 125, 29–54.
- Danielsen, E.F., 1993: In situ evidence of rapid, vertical irreversible transport of lower tropospheric air into the lower tropical stratosphere by convective cloud turrets and by large-scale upwelling in tropical cyclones. *J. Geophys. Res.*, 98, 8665–8681.
- Davidson, N.E., J.L. McBride, and B.J. McAvaney, 1983: The onset of the Australian monsoon during Winter MONEX: Synoptic aspects. *Mon. Wea. Rev.*, 111, 496–516.
- Davidson, N.E. and H.H. Hendon, 1989: Downstream development in the Southern Hemisphere monsoon during FGGE/WMONEX. *Mon. Wea. Rev.*, 117, 1458–1470.
- Drosowsky, W., 1996: Variability of the Australian summer monsoon at Darwin: 1957–1992. *J. Climate*, 9, 85–96.
- Frank, W.M. and J.L. McBride, 1989: The vertical distribution of heating in AMEX and GATE cloud clusters. *J. Atmos. Sci.*, 46, 3464–3478.
- Gill, A.E., 1980: Some simple solution for heat induced tropical circulations. *Quart. J. Roy. Meteor. Soc.*, 106, 447–462.
- Gray, W.M., 1979: Hurricanes: Their formation, structure and likely role in the tropical circulation. *Meteorology Over the Tropical Oceans*. D. B. Shaw (Ed.), Roy Meteor. Soc., UK, 155–218.
- Hall, J.D., A.J. Matthews, and D.J. Karoly, 2001: The modulation of tropical cyclone activity in the Australian region by the Madden-Julian oscillation. *Mon. Wea. Rev.*, 129, 2970–2982.
- Hendon, H.H., 2003: Indonesian rainfall variability: Impacts of ENSO and local air-sea interaction. *J. Climate*, 16, 1775–1790.
- Hendon, H.H., N.E. Davidson, and B. Gunn, 1989: Australian summer monsoon onset during AMEX 1987. *Mon. Wea. Rev.*, 117, 370–390.

- Hendon, H.H. and B. Liebmann, 1990a: A composite study of onset of the Australian summer monsoon. *J. Atmos. Sci.*, 47, 2227–2240.
- Hendon, H.H. and B. Liebmann, 1990b: The intraseasonal (30–50 day) oscillation of the Australian summer monsoon. *J. Atmos. Sci.*, 47, 2909–2923.
- Hendon, H.H., C. Zhang, and J.D. Glick, 1999: Interannual variation of the Madden-Julian oscillation during Austral Summer. *J. Climate*, 12, 2538–2550.
- Holland, G.J., 1986: Interannual variability of the Australian summer monsoon at Darwin: 1952–82. *Mon. Wea. Rev.*, 114, 594–604.
- Hung, C.-W. and M. Yanai, 2004: Factors contributing to the onset of the Australian summer monsoon. *Quart. J. Roy. Meteor. Soc.*, 130, 739–758.
- Hung, C.-W., X. Liu, and M. Yanai, 2004: Symmetry and asymmetry of the Asian and Australian summer monsoons. *J. Climate*, 17, 2413–2426.
- Joseph, P.V., B.Liebmann, and H.H.Hendon, 1991: Interannual variability of the Asutralian summer monsoon onset: possible influences of Indian summer monsoon and El Niño. *J. Climate*, 4, 529–538.
- Kawamura, R., Y. Fukuta, H. Ueda, T. Matsuura, and S. Iizuka, 2002: A mechanism of the onset of the Australian summer monsoon. *J. Geophys. Res.*, 107, No D14, 4204, 10.1029/2001JD001070, 2002.
- Keenan, T.D., and L.R. Brody, 1988: Synoptic-scale modulation of convection during the Australian summer monsoon. *Mon. Wea. Rev.*, 116, 71–85.
- Keenan, T.D. and R. E. Carbone, 1992: A preliminary morphology of precipitation systems in tropical northern Australia. *Quart. J. Roy. Meteor. Soc.*, 118, 283–326.
- Keenan, T.D. and S. A. Rutledge, 1993: Mesoscale characteristics of monsoonal convection and associated stratiform precipitation. *Mon Wea. Rev.*, 121, 352–374.
- Liebmann, B., H.H. Hendon, and J.D. Glick, 1994: The relationship between tropical cyclones of the western Pacific and Indian Oceans and the Madden-Julian oscillation. *J. Meteor. Soc. Japan.*, 72, 401–412.
- Love, G., 1985: Cross-equatorial influence of winter hemisphere subtropical cold surges. *Mon. Wea. Rev.*, 113, 1487–1498.
- Matsuno, T., 1966: Quasi-geostrophic motions in the equatorial area. *J. Meteor. Soc. Japan*, 44, 25–43.

- McBride, J.L., 1983: Satellite observations of the Southern Hemisphere monsoon during Winter MONEX. *Tellus*, 35A, 189–197.
- McBride, J.L. and W.M. Frank, 1999: Relationships between stability and monsoon convection. *J. Atmos. Sci.*, 56, 24–36.
- McBride, J.L. and N. Nicholls, 1983: Seasonal relationships between Australian rainfall and the Southern Oscillation. *Mon. Wea. Rev.*, 111, 1998–2004.
- McBride, J.L. and T.D. Keenan, 1982: Climatology of tropical cyclone genesis in the Australian region. *J. Climatol.*, 2, 13–33.
- Nicholls, N., 1981: Air-sea interaction and the possibility of long-range weather prediction in the Indonesian Archipelago. *Mon. Wea. Rev.*, 109, 2435–2443.
- Nicholls, N., J.L. McBride, and R.J. Ormerod, 1982: On predicting the onset of the Australian wet season at Darwin. *Mon. Wea. Rev.*, 110, 14–17.
- Slingo, J.M., D.P. Rowell, K.R. Sperber, F. Nortley, 1999: On the predictability of the interannual behaviour of the Madden-Julian oscillation and its relationship with El Niño. *Quart. J. Roy. Meteor. Soc.*, 125, 583–609.
- Sumathipala, W.L. and T. Murakami, 1988: Intraseasonal fluctuations in low-level meridional winds over the south China Sea and the western Pacific and monsoonal convection over Indonesia and northern Australia, *Tellus*, A, 40, 205–219.
- Troup, A.J., 1961: Variations in upper tropospheric flow associated with the onset of the Australian summer monsoon. *Indian J. Meteor. Geophys.*, 12, 217–230.
- Wang, B., R. Wu, and T. Li, 2003: Atmosphere-warm ocean interaction and its impact on Asian-Australian monsoon variation. *J. Climate*, 16, 1195–1211.
- Wheeler, M.C., and J. L. McBride, 2004: Intraseasonal Variability of the Australian-Indonesian Monsoon Region. In *Intraseasonal Variability of the Atmosphere-Ocean Climate System*, W. K.-M. Lau and D. E. Waliser Eds., Praxis Publishing.
- Wheeler, M.C. and H.H. Hendon, 2004: An all-season real-time multivariate MJO index: Development of an index for monitoring and prediction. *Mon. Wea. Rev.*, (in press).
- Wheeler, M., G.N. Kiladis, and P.J. Webster, 2000: Large-scale dynamical fields associated with convectively coupled equatorial waves. *J. Atmos. Sci.*, 57, 613–640.
- Yano, J.I., and J.L. McBride, 1998: An aqua planet monsoon. *J. Atmos. Sci.*, 55, 1373–1399.

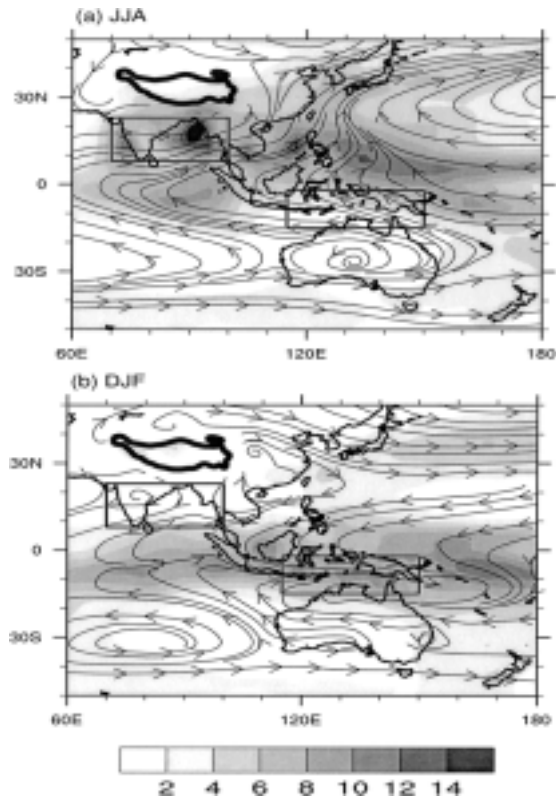


Figure 1 Mean streamlines at 850mb (contours) and precipitation (shaded, mm/day) for JJA and DJF. From Hung et al. 2004

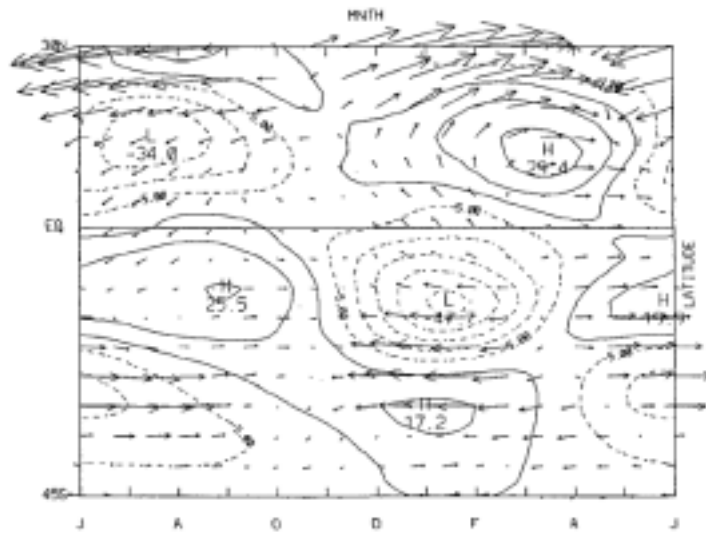


FIG. 2. First three harmonics of the annual cycle (annual, semiannual, terannual) of OLR (contoured) and ECMWF 200 mb winds (vectors) averaged between 130–145 E. Contour interval is 10 W m^{-2} (first contour at $\pm 5 \text{ W m}^{-2}$) and maximum vector wind has magnitude 30 m s^{-1} . See text for details.

Figure 2 First three harmonics of annual cycle of OLR (contour) and 200 mb winds (vectors) averaged in the Australian sector (130-145E). From Hendon and Liebmann 1990.

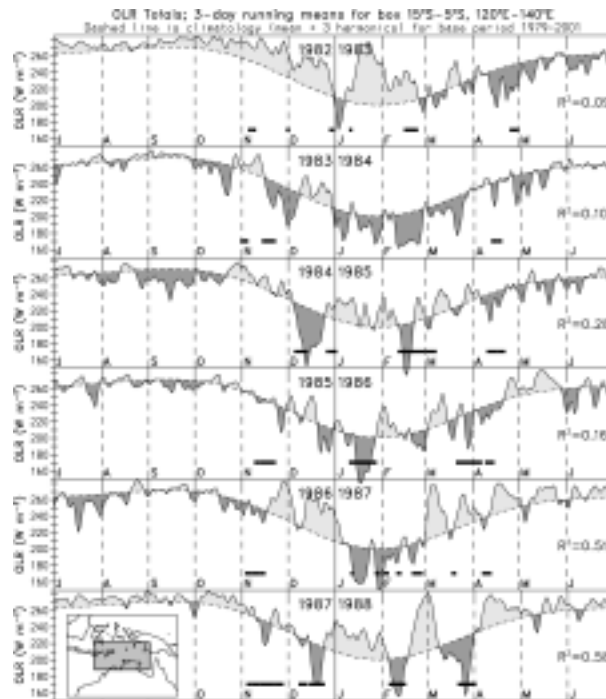


Figure 3 From Wheeler and McBride 2004. OLR averaged to north of Australia (box given in insert). Dashed lines mean seasonal cycle. Heavy bars indicate periods of active convection associated with the MJO, as

determined by CEOF analysis of equatorial averaged OLR and zonal wind at 850mb and 200mb. R^2 values are explained OLR variance in the boxed region for each summer monsoon season by the MJO.

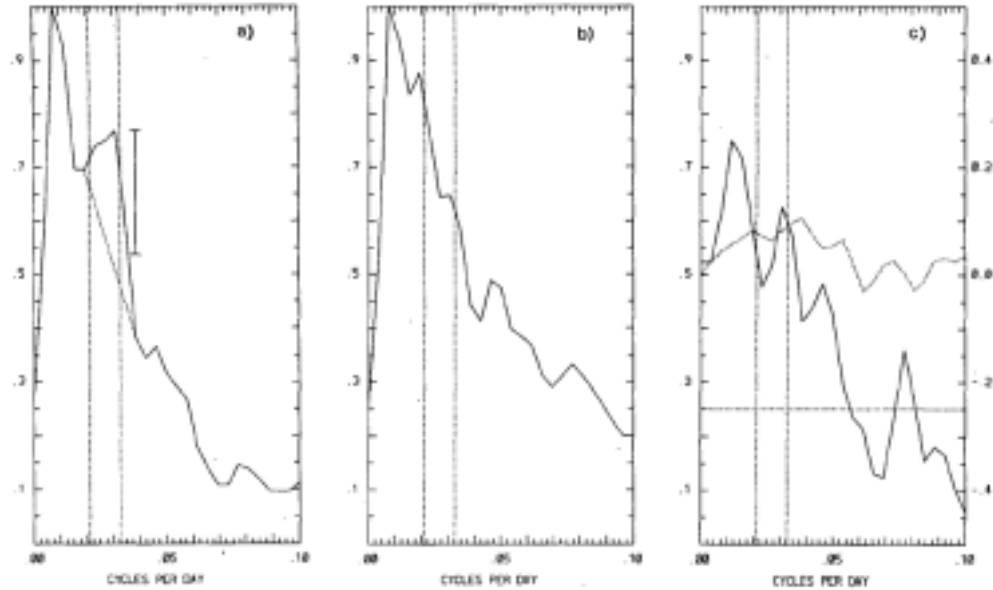


FIG. 2. Power spectra of (a) U_{10a} at Darwin and (b) North Australian rainfall for the summer seasons (15 October–15 April) 1957–87. The power has been normalized to unity and only frequencies less than 0.1 cycles per day are shown. The vertical lines demark the "30–50" day period range (frequency band 5.5/256–8.5/256 cpd). The 95% confidence limit (assuming 62 degrees of freedom) for the spectral peak at 32 day period and the bandwidth (1/256 cpd; horizontal bar) are shown in (a). A subjective estimate of the background spectrum in (a) was made by the linear fit between the adjacent spectral minima to the 30–50 day band (dashed line). (c) The coherence squared (solid) and phase (dashed) between U_{10a} and North Australian rainfall. The scale for coherence squared is on the left and phase angle (in cycles) is on the right. A positive phase indicates rainfall leads U_{10a} . The horizontal line is the 95% confidence limit (assuming 62 degrees of freedom) for the coherence squared estimate.

Figure 4 From Hendon and Liebmann 1990b

MJO composite for December-January-February

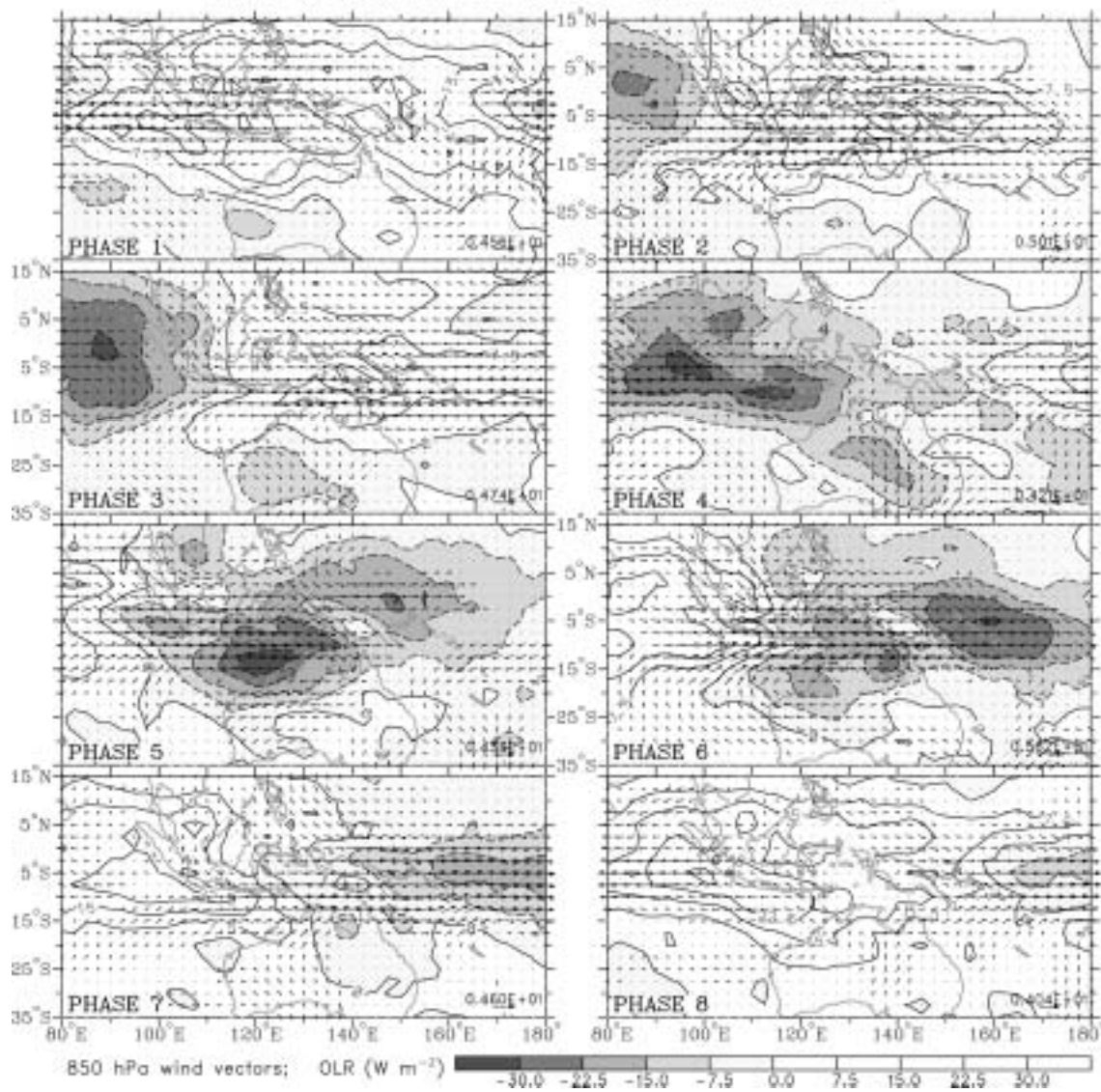


Figure 5: Compositing OLR and 850-hPa wind anomalies for eight phases of the MJO during December-January-February (DJF). OLR contour interval is 7.5 W m^{-2} , with negative contours dashed and negative values shaded. Black vectors indicate wind anomalies that are statistically significant at the 99% level, based on their local standard deviation and the Student's t test. Grey vectors do not pass the 99% level test. The magnitude of the largest vector is shown on bottom-right of each panel. From Wheeler and Hendon 2004

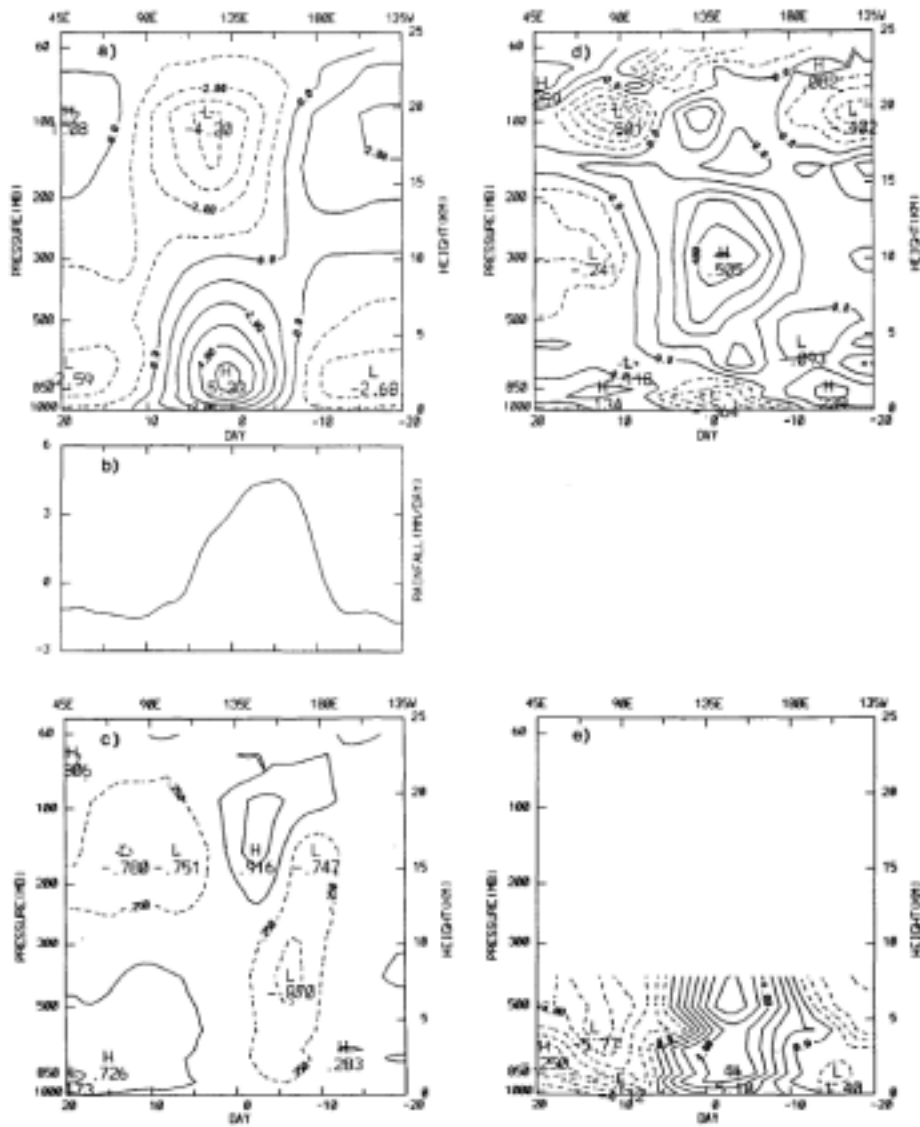


FIG. 5. Composite 30-50 day oscillation (91 events) at Darwin of (a) zonal wind, (b) rainfall, (c) meridional wind, (d) temperature, and (e) relative humidity. Unfiltered fields were composited. The contour intervals are (a) 1 m s^{-1} , (c) 0.5 m s^{-1} (first contour at $\pm 0.25 \text{ m s}^{-1}$), (d) 0.1°K , and (e) 1.0% . Composites run from -20 days to +20 days with day zero corresponding to the maximum 850 mb westerly wind. Note time runs from right to left. The longitudinal scale across the top of the figures is an approximate one assuming that the composited oscillation moves steadily outward at 4 m s^{-1} . The height scale was approximated hydrostatically from the pressure level using a constant scale height of 8.5 km.

Figure 6 From Hendon and Liebmann 1990b

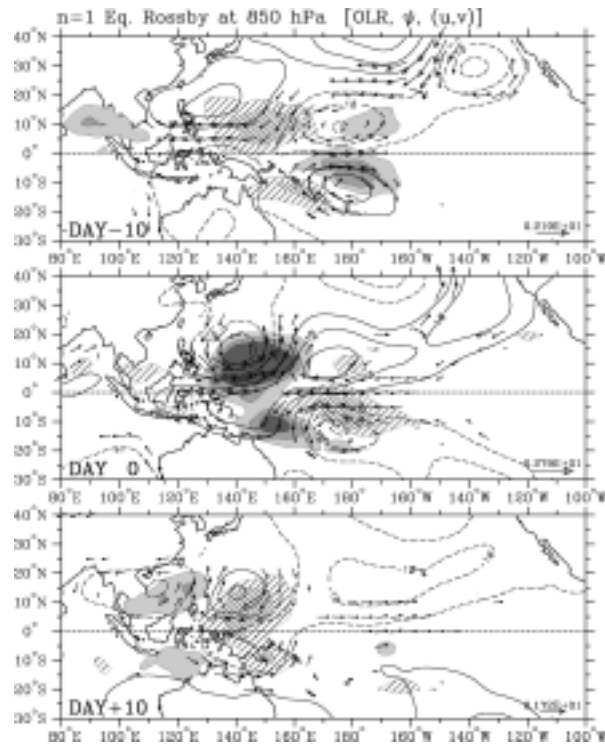


Figure 7: Horizontal structure of a $n=1$ equatorial Rossby (ER) wave over a sequence spanning 21 days, as computed using lagged regression based on a two standard deviation anomaly in the ER wave filtered OLR series at 10°S , 150°E . Shading/cross-hatching show the negative/positive OLR anomalies at the levels of -15, -10, -5, 5, and 10 W m^{-2} . Contours are streamfunction at the 850 hPa level (interval of $5 \times 10^5 \text{ m}^2 \text{ s}^{-1}$), with negative contours dashed and the zero contour omitted. Vectors are the 850-Pa wind anomalies, plotted only where the local correlation of either wind component is statistically significant at the 99% level. [Reproduced from Wheeler et al. (2000).]

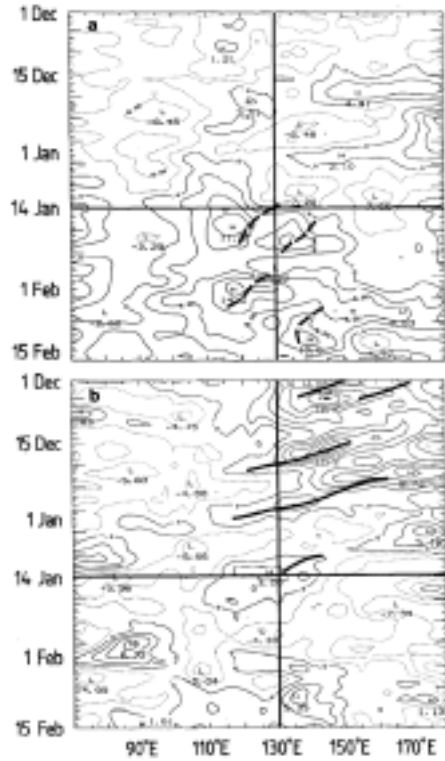


FIG. 10. Longitude-time series of daily 850 mb zonal wind at (a) 10°S and at (b) the equator. Contour interval is (a) 4 $m s^{-1}$ and is (b) 2 $m s^{-1}$. Solid horizontal and vertical lines indicate the approximate location of the AABDC region (130°E) and date of onset, 14 January 1987. Heavy dashed lines are southern hemisphere cyclone tracks (between 7° and 17°S) while heavy solid lines are for Northern Hemisphere cyclones.

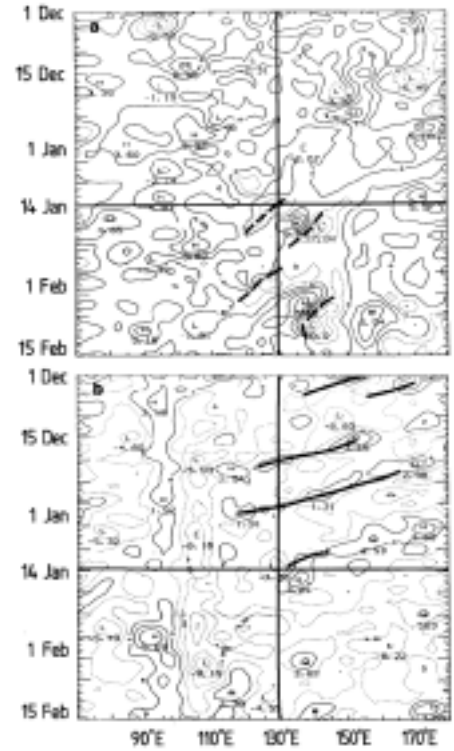


FIG. 11. As in Fig. 10 except for 850 mb meridional wind at (a) 10°S and at the equator (b). The contour interval is 2 $m s^{-1}$.

Figure 8 Zonal wind at 850 mb along 10S (top) and Eq (bottom) for 1 Dec 1986 – 15 Feb 1987. Heavy dashed (solid curves) are southern (northern) hemisphere cyclone tracks. Heavy horizontal line indicates onset date at Darwin (heavy vertical line) From Hendon and Liebmann (1990)

Figure 9 As in Fig. 8 except for meridional wind at 850 mb.

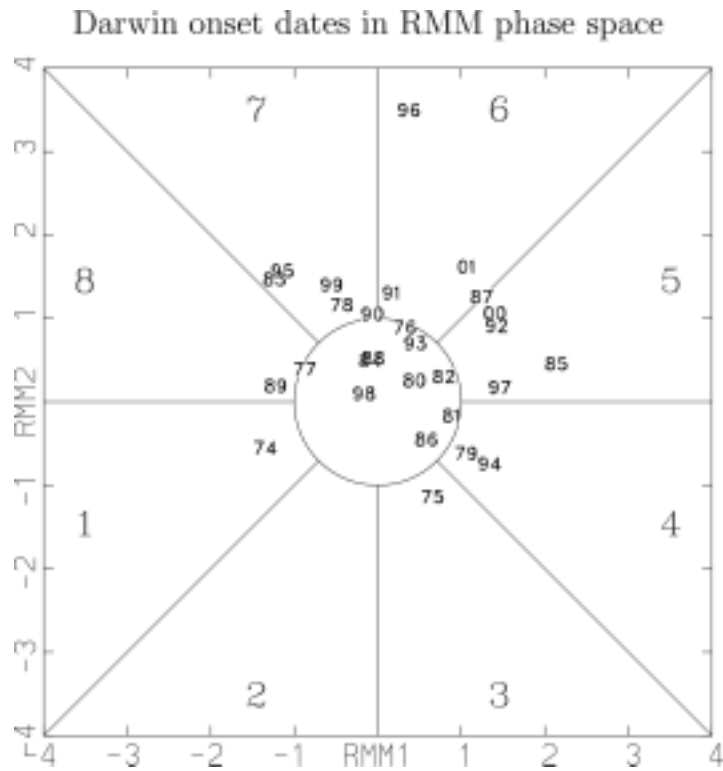


Figure 12: Onset date each year as a function of the state of the MJO, given by the projection onto the leading CEOFs of equatorially averaged OLR, and zonal wind at 200 and 850 mb. Onset dates are based on the daily deep-layer mean zonal wind, at Darwin, Australia as given by Drosowsky (1996). Reproduced from Wheeler and Hendon (2004).

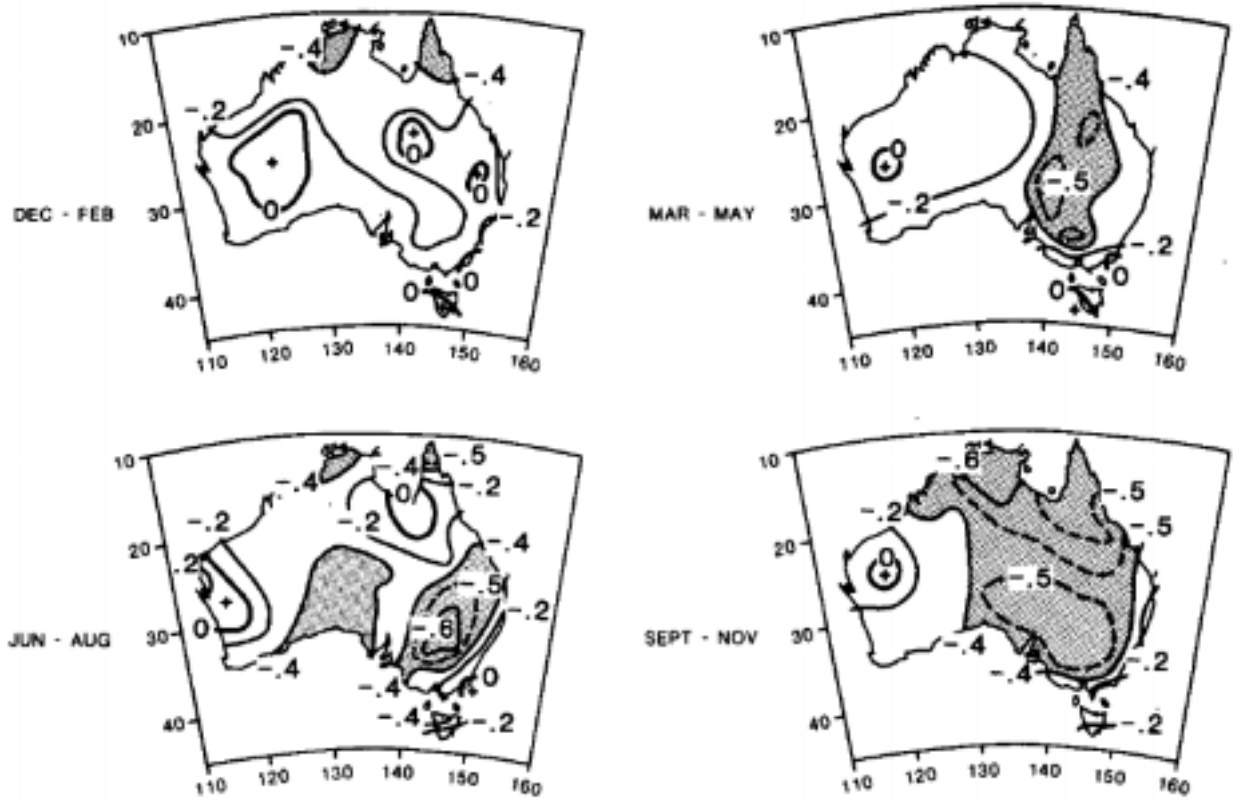


FIG. 2. Simultaneous correlations between Darwin pressure and district rainfall for the four seasons, December-February, March-May, June-August, September-November. Data from 1932-74.

Figure 13 From McBride and Nicholls 1983

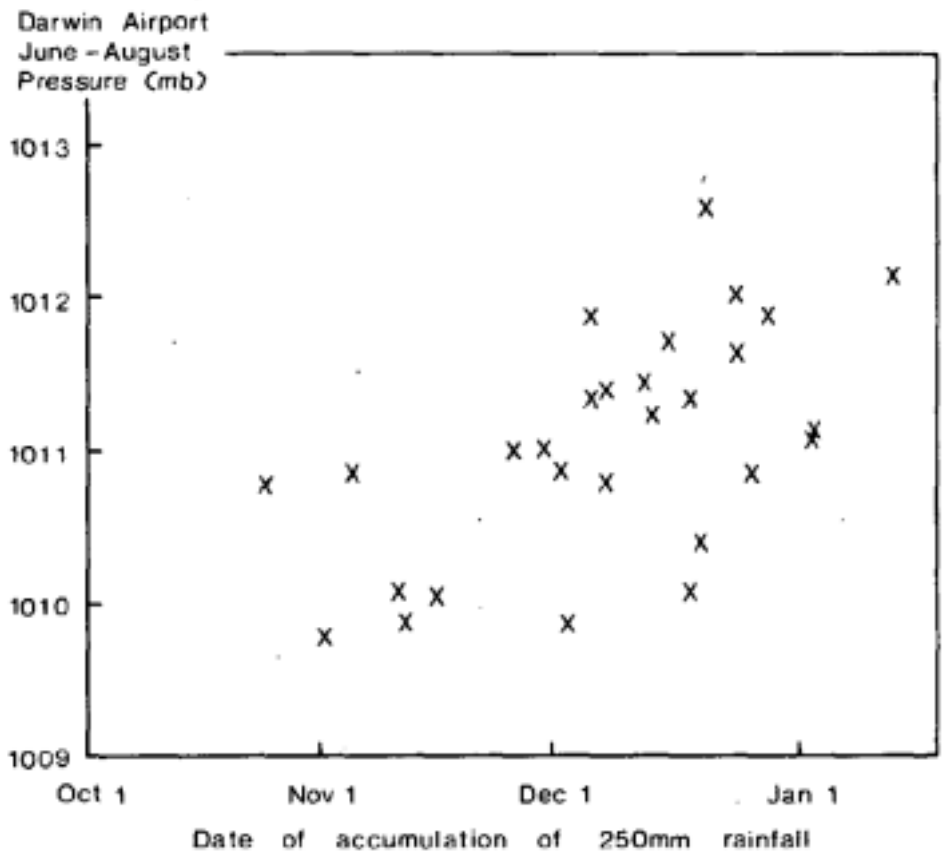


FIG. 2. Scatter diagram of Darwin Airport June-August pressure versus the date by which 250 mm rainfall has accumulated. Data from 1952-80.

Figure 14 Nicholls et al. 1982

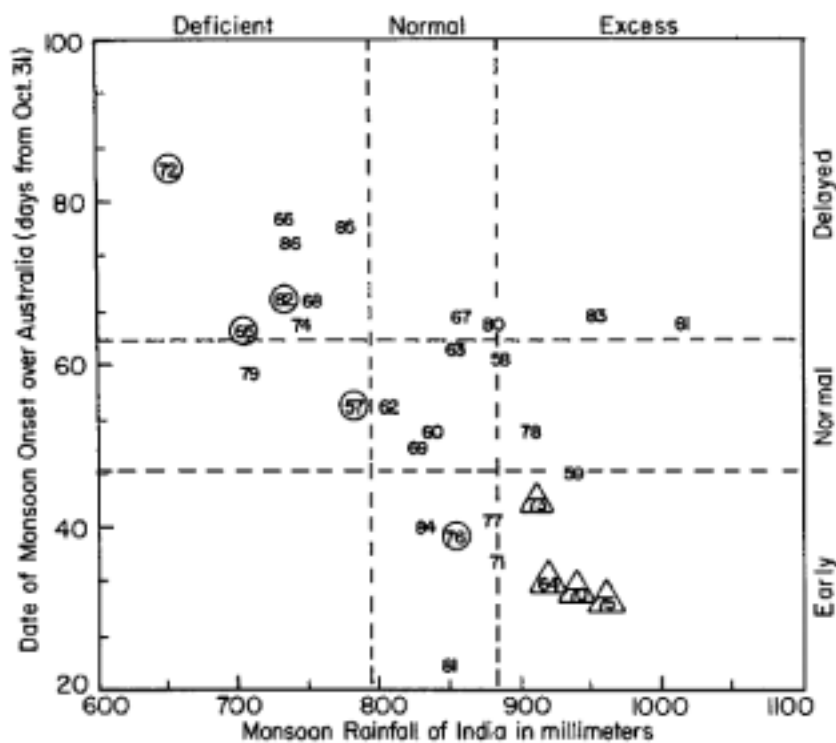


FIG. 2. Scatter diagram between June to September ISMR in millimeters for each of the 30 years 1957-1986 and the date of the following ASMO. ASMO counted as days from 31 October (i.e., 1 November is day 1). Last two digits of year of ISMR mark the location. Each axis is divided into categories of one-half standard deviation and more above the mean, normal, and one-half standard deviation and more below the mean. El Niño years are circled and cold event years are triangled.

Figure 15 From Joseph et al. 1991

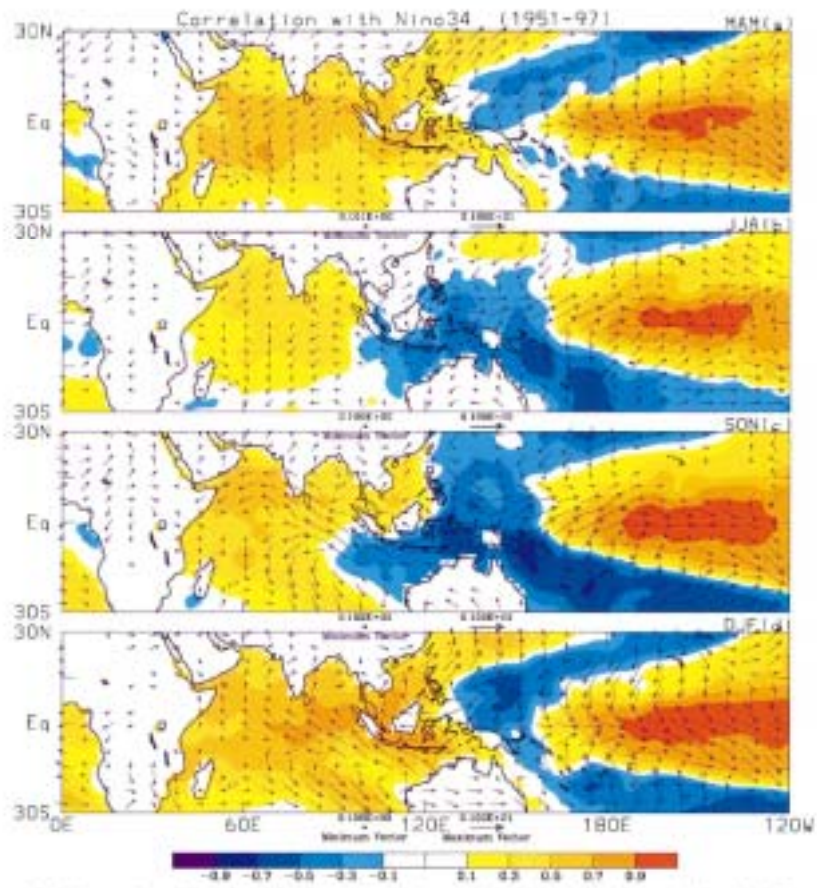


FIG. 5. Seasonal correlation of Niño-3.4 with SST and surface winds for (a) MAM, (b) JJA, (c) SON, and (d) DJF. Plotting convention is same as in Fig. 4.

Figure 16 From Hendon 2003

Table 1 From Nicholls et al. 1982

TABLE 4. Correlations between the onset indices and Darwin wet-season rainfall. The last row shows correlations between June–August pressure and seasonal rainfall. (The 5% significance level occurs at a correlation of 0.374.)

	Darwin rainfall		
	Sep–May	Sep–Nov	Dec–May
Date of 1st 10 mm	–0.267	–0.477	–0.084
Date of 1st 50 mm	–0.383	–0.707	–0.111
Date of 1st 100 mm	–0.289	–0.817	0.034
Date of 1st 250 mm	–0.394	–0.905	–0.040
Date of 1st 500 mm	–0.520	–0.819	–0.209
Darwin pressure: June–August	–0.335	–0.661	–0.079